Impaired FGF signaling contributes to cleft lip and palate

Bridget M. Riley*, M. Adela Mansilla*, Jinghong Ma†, Sandra Daack-Hirsch*, Brion S. Maher‡, Lisa M. Raffensperger*, Erilynn T. Russo*, Alexandre R. Vieira‡, Catherine Dodé§, Moosa Mohammadi†, Mary L. Marazita‡¶, and Jeffrey C. Murray*‖

*Department of Pediatrics, University of Iowa, Iowa City, IA 52242; †Department of Pharmacology, New York University School of Medicine, New York, NY 10016; ‡Center for Craniofacial and Dental Genetics, Department of Oral Biology, School of Dental Medicine, University of Pittsburgh, Pittsburgh, PA 15219; §Institut Cochin et Laboratoire de Biochimie et Génétique Moléculaire, Hôpital Cochin, 75014 Paris, France; and ¶Department of Human Genetics, Graduate School of Public Health, University of Pittsburgh, Pittsburgh, PA 15219

Edited by Mary-Claire King, University of Washington, Seattle, WA, and approved January 18, 2007 (received for review September 12, 2006)

Nonsyndromic cleft lip and palate (NS CLP) is a complex birth defect resulting from a combination of genetic and environmental factors. Several members of the FGF and FGFR families are expressed during craniofacial development and can rarely harbor mutations that result in human clefting syndromes. We hypothesized that disruptions in this pathway might also contribute to NS CLP. We sequenced the coding regions and performed association testing on 12 genes (*FGFR1*, *FGFR2*, *FGFR3*, *FGF2*, *FGF3*, *FGF4*, *FGF7*, *FGF8*, *FGF9*, *FGF10*, *FGF18*, and *NUDT6*) and used protein structure analyses to predict the function of amino acid variants. Seven likely disease-causing mutations were identified, including: one nonsense mutation (R609X) in FGFR1, a *de novo* missense mutation (D73H) in FGF8, and other missense variants in FGFR1, FGFR2, and FGFR3. Structural analysis of FGFR1, FGFR2, and FGF8 variants suggests that these mutations would impair the function of the proteins, albeit through different mechanisms. Genotyping of SNPs in the genes found associations between NS CLP and SNPs in *FGF3*, *FGF7*, *FGF10*, *FGF18*, and *FGFR1*. The data suggest that the FGF signaling pathway may contribute to as much as 3–5% of NS CLP and will be a consideration in the clinical management of CLP.

fibroblast growth factor | fibroblast growth factor receptor | single-nucleotide polymorphism | cleft palate

Isolated or nonsyndromic cleft lip and palate (NS CLP) is a common congenital anomaly affecting ≈1/700 live births worldwide, although prevalence varies widely based on geographic and socioeconomic status (1, 2). Significantly increased lifetime mortality ratios of 1.4 for males and 1.8 for females are associated with NS CLP (3). Additionally, clefting requires extensive medical interventions that create significant economic and social burdens for family and society (4).

Both genetic and environmental factors are known to play a role in the development of NS CLP, complicating the identification of causal genes. A study examining recurrence patterns of NS CLP estimated that as many as 14 interacting loci may be involved in clefting (5). Prior sequencing analysis of DNA samples from NS CLP cases has indicated minor roles for mutations in MSX1, FOXE1, GLI2, MSX2, SKI, and SPRY2 in the etiology of NS CLP (6–8). Additionally, polymorphisms in the IRF6 gene have been found to be strongly associated with NS CLP, accounting for ≈12% of clefting (9).

Mammalian fibroblast growth factors (FGF1–FGF10 and FGF16–FGF23) control a wide spectrum of biological functions during development and adult life (10). The biological activities of FGFs are conveyed by seven principal FGF receptor tyrosine kinases encoded by four distinct genes (*FGFR1–FGFR4*). In the presence of heparan sulfate proteoglycans, two FGFs bind to two FGFRs, inducing receptor dimerization and enabling the intracellular tyrosine kinase domains to transphosphorylate and become activated (11). Human diseases that arise from dysregulated FGF signaling include craniosynostosis and skeletal dysplasia syndromes (FGFR1–FGFR3) and Kallmann syndrome (KS) (FGFR1). Cleft palate occurs in 44% of cases of Apert syndrome, which is characterized by combined craniosynostosis and syndactyly (12, 13). Two mutations in the FGFR2 gene, S252W and P253R, account for almost all cases of Apert syndrome; the clefting phenotype is more commonly associated with the S252W mutation (59%) than with the P253R mutation (17%) (12, 14). The autosomal-dominant KS, whose main features are anosmia and hypogonadotrophic hypogonadism, is caused by loss-of-function mutations in FGFR1, and 5–10% of these patients have a cleft (unpublished estimate) (15–17). Additionally, mutations in FGF10 are associated with autosomal-dominant aplasia of lacrimal and salivary glands (18).

Animal models also support the involvement of FGFs and FGFRs in the pathogenesis of CLP. $Fgf10^{-/-}$ (19), $Fgfr2b^{-/-}$ (20), $Fgf18^{-/-}$ (21, 22), and Fgfr1 hypomorphic mice have cleft palate (23). Hypomorphic $Fgf8^{neo/-}$ mutant mice have craniofacial defects, including abnormal development of the palate and palatine bones (24). Moreover, disruption of the directional epithelial-mesenchymal Fgf10-Fgfr2b signaling has been found to result in cleft palate in mice (19). In this report, we provide direct sequencing and association data showing that disruptions in FGF signaling also contribute to CLP in humans.

Results

Sequencing. Overall, 84 amplicons encoding ≈33,000 base pairs were sequenced for the 12 FGF and FGFR genes in genomic DNA for 184 individuals with NS CLP [see supporting information (SI) Table 3]. Thirty-seven point mutations were identified in the exons or at the intron–exon junctions of the *FGF* and *FGFR* genes examined in families with NS CLP from both Iowa (16) and the Philippines (20). All mutations appear in SI Table 4, and the nine missense and nonsense mutations are listed in Table 1. SI Table 5 contains the predictions from exon splice-enhancer programs on the effects of the synonymous mutations identified in the coding regions. None of these mutations has been previously reported in the SNP database (dbSNP). When we excluded from the analysis the initial ascertainment cases and

Author contributions: B.M.R. and J.C.M. designed research; B.M.R., M.A.M., J.M., S.D.-H., B.S.M., L.M.R., E.T.R., A.R.V., M.M., and M.L.M. performed research; C.D. contributed new reagents/analytic tools; B.M.R., M.A.M., B.S.M., L.M.R., E.T.R., A.R.V., M.M., M.L.M., and J.C.M. analyzed data; and B.M.R., M.M., M.L.M., and J.C.M. wrote the paper;.

The authors declare no conflict of interest.

This article is a PNAS direct submission.

Freely available online through the PNAS open access option.

Abbreviations: FGFR, fibroblast growth factor receptor; KS, Kallmann syndrome; NS CLP, nonsyndromic cleft lip and palate.

‖To whom correspondence should be addressed: Email: jeff-murray@uiowa.edu.

This article contains supporting information online at www.pnas.org/cgi/content/full/0607956104/DC1.

Table 1. Missense and nonsense mutations in FGF pathway genes identified in NS CLP patients

Gene	Mutation	Population	Phenotype	Frequency	Control frequency	UCSC browser position*
FGFR1	M369I	Philippine	CPO UL CLP	2/1117	0/1368	Chr 8: 38,396,385
FGFR1	E467K	Philippine	UL CLP	2/1117	0/1384	Chr 8: 38,394,934
FGFR1	R609X	Iowa	UL CLP BL CLP	1/90	0/91	Chr 8: 38,392,574
FGFR2	D138N	Philippine	UL CLP BL CLP	5/1027	0/1392	Chr 10: 123,314,048
FGFR2	R84S	Iowa	BL CLP	1/362	0/1328	Chr 10: 123,315,066
FGFR3	V329I	Philippine	UL CL UL CLP BL CLP	8/977	5/961	Chr 4: 1,772,704
FGF8	D73H (*de novo*)	Iowa	BL CLP	1/262	0/1110	Chr 10: 103,524,599
FGF10	S59F	Philippine	BL CLP	2/91	3/83	Chr 5: 44,424,366
NUDT6	K172N	Iowa	Untyped CLP	1/87	0/89	Chr 4: 124,1276,421

CPO, cleft palate only; UL, unilateral; BL, bilateral; CL, cleft lip; CLP, cleft lip and palate; Untyped, cleft lip laterality unknown.
*UCSC browser position from the May 2004 assembly.

did a formal case-control study looking for the presence of M369I, E467K, R84S, D138N, V329I, and D73H, we found a significant difference between mutations in cases versus controls ($P = 0.04$). The protein sequence-altering mutations are more common in cases of NS SLP than in controls.

Two FGFR1 mutations, M369I and E467K, were identified in pedigrees from the Philippines. The M369I mutation was found in two unrelated families (SI Fig. 6). One family had three affected siblings, as well as one unaffected sibling and an unaffected mother, each with the mutation. The father was unavailable, but a paternal brother with a cleft did not have the mutation. The E467K mutation was also found in cases from two unrelated families (SI Fig. 7). In one family, the E467K was found in one affected member but was absent in their first cousin with a cleft. These mutations were not seen in the 1,064 members of the Human Diversity Cell Line Panel (25) or in 328 additional controls without clefts from the Philippines. The R609X nonsense mutation in FGFR1 was found in an individual who was originally seen at age 12 and diagnosed with an isolated CLP. At age 16, she was self-diagnosed with anosmia and presented with irregular menstrual periods, a missing upper right canine, and a missing upper left first premolar (all reported features of KS). Her father presented with an isolated CLP, had the R609X mutation, and was fertile (no hormonal testing done), with a normal sense of smell. This mutation was not present in either the unaffected mother or in the brother who had operated pulmonic stenosis (Fig. 1). A deceased paternal great aunt was also reported to have a cleft lip.

The M369I mutation maps to the extracellular juxtamembrane domain, the linker sequence between Ig-like (Ig) domain III (D3) and the transmembrane helix, whereas the E467K mutation maps to the intracellular juxtamembrane domain that links the transmembrane helix to the tyrosine kinase domain of FGFR1. Both the M369 and E467 are conserved among the human, chimp, mouse, rat, and chicken protein sequences (Fig. 2*B*). In the crystal structure of the FGFR1 kinase domain, E467 is completely solvent-exposed and does not participate in the overall folding of the FGFR1 kinase domain (Fig. 2*A*). Interestingly, however, E467 is located four residues C terminal to Y463, one of the main tyrosine phosphorylation sites of FGFR1. Phosphorylated Y463 has been implicated in the binding and phosphorylation of the SH2 containing signaling molecules such as Crk and is part of the recognition sequence Y-E-L-P, a preferred binding motif for Crk SH2 domain (26, 27). Additionally, when the FGFR1 Y463F mutant is expressed in cells, it is unable to proliferate in response to FGF2, indicating its role in cell proliferation (27). Based on the proximity of the E467K mutation to Y463, we predict that this mutation should impact recruitment and phosphorylation of this downstream signaling. The R609X nonsense mutation maps onto helix αE in the FGFR1 tyrosine kinase domain and represents a loss-of-function mutation because this mutation will delete a catalytically essential portion of the FGFR1 tyrosine kinase domain. Alternatively,

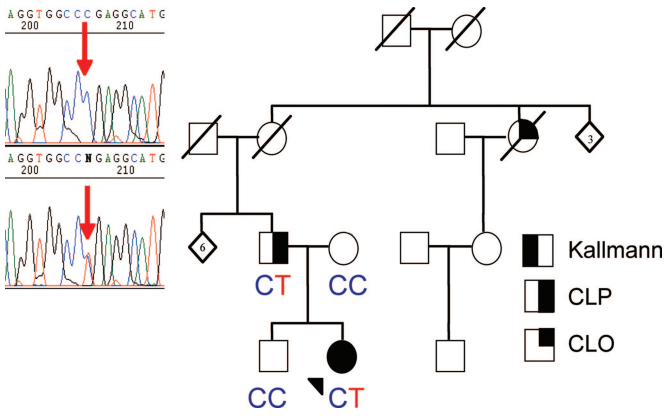

Fig. 1. R609X pedigree. This pedigree demonstrates mixed phenotypes, with the father presenting as NS CLP only, while his daughter had KS with CLP. Both father and daughter were heterozygous for the R609X mutation.

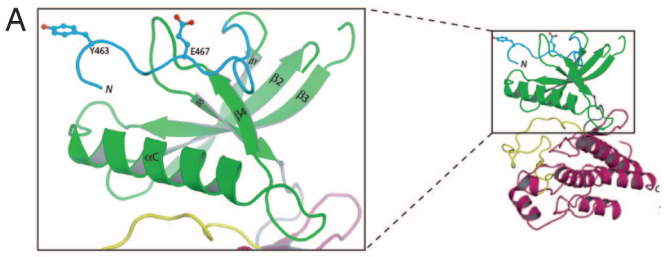

Fig. 2. FGFR1 mutations. (*A*) The location of E467 is mapped onto the crystal structure of FGFR1 kinase domain. The coloring of the intracellular tyrosine kinase domain is as follows: the N-terminal lobe of kinase in green, the C-terminal lobe in purple, the activation loop in yellow, and the kinase hinge region in gray. Note that ATP (not shown) binds in the cleft between the N-lobe and C-lobe of the kinase domain. E467 is located near the Y463 autophosphorylation site. Atom coloring is as follows: nitrogen in blue, oxygen in red, and sulfur in yellow. Hydrogen bonds are shown as dashed lines. N, N terminus; C, C terminus. (*B*) Conservation of FGFR1 mutations. CLUSTALW alignment of vertebrate FGFR1s and human FGFRs.

GENETICS

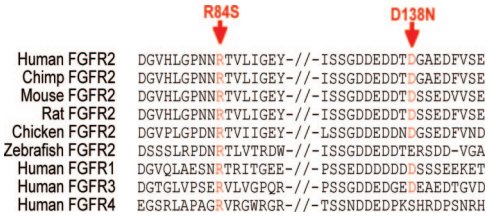

Fig. 3. Conservation of FGFR2 mutations. CLUSTALW alignment of vertebrate FGFR2s and human FGFRs.

this mutation may cause haploinsufficiency because mRNAs with premature termination codons can be targeted to nonsense-mediated decay (28).

The R84S missense mutation was found in the FGFR2 gene of an individual from Iowa with bilateral CLP and no history of CLP on either side of the family. This mutation was found in 1 case of 362 Iowa cleft cases and was absent in 290 Iowa controls and the 1,064 members of the Human Diversity Cell Line Panel (25). Because no DNA sample is available from her unaffected parents or sister, we cannot know whether the mutation was transmitted from unaffected parents or *de novo*. R84S resides in the Ig domain 1 (D1) of FGFR2 and is conserved between human and zebrafish FGFR2 sequences, as well as between human FGFR1 and FGFR4 (Fig. 3). In the recently reported solution structure of the murine FGFR1 D1, the side chain of the homologous arginine residue is solvent-exposed and does not play any role in the structural identity of D1 (29). Although the R84S mutation is not expected to impair folding of D1, it may still alter the extent of autoinhibition mediated by D1. In the autoinhibitory state, the D1 and D1–D2 linker regions fold over and prevent FGF and heparin binding to the D2–D3 domains (11). FGFR1 mutations in the D1 domain and D1–D2 linker/acid box domain augment the autoinhibitory state of FGFR1, leading to the loss of function in KS patients (11) and supporting R84S as a functional mutation.

The D138N mutation located in the D1–D2 linker/acid box domain of FGFR2 was originally found in a Filipino individual with CLP. Screening of the 1,027 Philippine NS CLP cases found 4 more CLP individuals with the D138N mutation. Zero of 328 Philippine controls and 0 of 1,064 members of the Human Diversity Cell Line Panel (25) had the variant. The aspartic acid residue is conserved among human, mouse, rat, chicken, and frog, but not zebrafish, and in human FGFR1 and FGFR3 (Fig. 3). As stated above, the D1–D2 linker/acid box domain is also critical for FGFR autoinhibition. We predict that, like the R84S mutation, the D138N mutation in FGFR2 may also influence the degree of receptor autoinhibition.

The V329I mutation in FGFR3 was discovered in a Filipino individual with bilateral CLP and microphthalmia, as well as in her unaffected mother. There was a negative family history for clefting. The V329I mutation maps to the Ig domain III (D3) of FGFR3, and structural analysis data predict that this mutation should destabilize the tertiary folding of D3 (Fig. 4*A*). The aliphatic side chain of V329 points into the hydrophobic core of D3 at the membrane proximal end of this domain. Substitution of V329 with the isoleucine, which has a slightly larger aliphatic side chain, should cause spatial conflicts with other hydrophobic residues in the inner core of D3, leading to a gradual unfolding of D3 and resulting in incomplete processing/maturation and retention of the mutated FGFR3 in the endoplasmic reticulum or other intracellular compartments. The valine at this position is strongly conserved between species (Fig. 4*B*), and all four FGFRs (Fig. 4*B*) indicate that this site is of functional importance.

An individual from Iowa with bilateral CLP harbored the D73H missense mutation in the FGF8 gene. Neither parent had

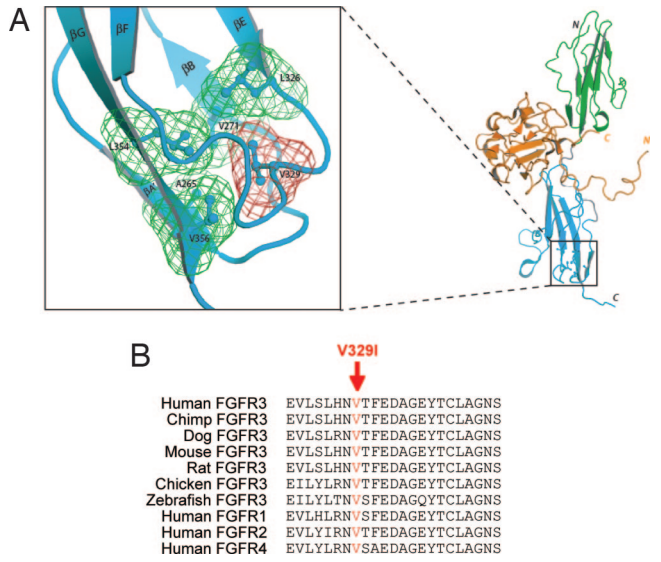

Fig. 4. FGFR3 mutation. (*A*) The position of V329 of FGFR3c is mapped onto the ribbon diagram of FGF1-FGFR3c complex. FGF is colored orange and the extracellular ligand binding region of FGFR3c is colored as follows: D2 in green, D3 in cyan, and the short D2–D3 linker in gray. The aliphatic side chain of V329 in FGFR3c points into the hydrophobic interior of D3 and thus contributes to the tertiary fold of the D3 core. To emphasize this observation, the surface of V329 is shown in red mesh, and the surface of hydrophobic residues that interact with V329 is rendered in green mesh. (*B*) Conservation of FGFR3 mutation. CLUSTALW alignment of vertebrate FGFR3s and human FGFRs.

the variant allele, suggesting that this mutation arose *de novo* (SI Fig. 8). Eighty SNP markers from different chromosomes were tested for this family, and no non-Mendelian inheritance errors were detected between the child and parents. Using these SNP markers and the EASYPAT program, a likelihood ratio of maternity/paternity vs. nonmaternity/paternity was calculated to be 1.34×10^7, supporting the conclusion that this child had a *de novo* mutation. The aspartic acid residue is conserved among human, chimp, rat, mouse, chicken, zebrafish, and puffer fish (Fig. 5*B*). Structural analysis data indicate that the D73H mutation is a loss-of-function mutation (Fig. 5*A*). The side chain of D73 makes three hydrogen bonds with the FGFR, and therefore the D73H mutation should reduce the binding affinity of FGF8 isoforms to their cognate FGFRs. Additionally, D73 makes several intramolecular bonds that facilitate the conformation of the FGF8 N terminus, thus the D73H mutation will destabilize the N-terminal conformation, which is important for receptor binding affinity and specificity (30).

The nucleoside diphosphate-linked moiety × motif 6 (NUDT6) gene is described as the antisense gene for FGF2 and may regulate FGF2 expression. Although the literature described this gene as a potential antisense transcript, the UCSC genome browser and NCBI (NP-009014) both have predicted the protein sequence for the gene. Additionally, the NUDT6 protein (also referred to as GFG) has been identified in human pituitary tumors, possibly representing a novel mechanism for regulating tumor cell growth (31). The K172N mutation was found in an individual from Iowa with CLP; however, there was no family history of clefting and no familial DNA available. The lysine is conserved among human, chimp, dog, rabbit, mouse, rat, chicken, and frog. Due to the lack of information about this gene, it is difficult to predict the potential functional consequences of the K172N mutation, yet it is of note that the mutation overlaps with the 3′ UTR of the FGF2 gene and is located in a region of high-nucleotide conservation.

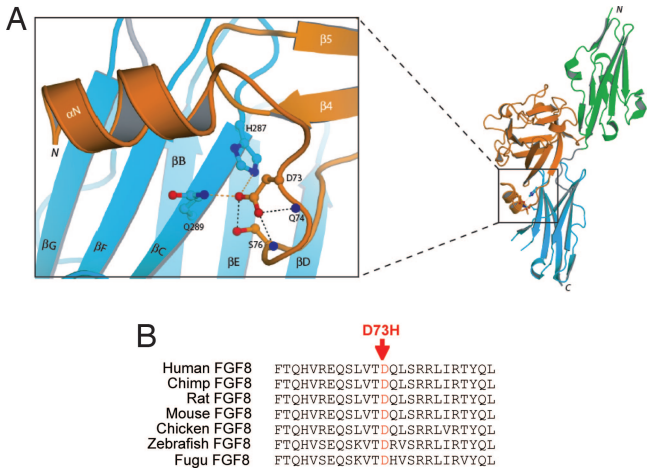

Fig. 5. FGF8 mutation. (*A*) The location of D73 in FGF8 is depicted onto the molecular structure of the FGF8b–FGFR2c complex. FGF is colored orange and the extracellular ligand binding region of FGFR2c is colored as follows: D2 in green, D3 in cyan, and the short D2–D3 linker in gray. Atom coloring is as follows: nitrogen in blue, oxygen in red, and sulfur in yellow. Hydrogen bonds are shown as dashed lines. N, N terminus; C, C terminus. The hydrogen bonds that D73 makes with the FGFR2 receptor residues Q289 and H287, as well as with FGF8 residues Q74 and S76, are indicated. (*B*) Conservation of FGF8 mutation. CLUSTALW alignment of vertebrate FGF8s.

Association. Family-Based Association Test (32, 33) analysis was performed on 294 multiplex, NS CLP Filipino families for two to four SNP markers in each of the following genes: *FGF2*, *FGF3*, *FGF4*, *FGF7*, *FGF8*, *FGF9*, *FGF10*, *FGF18*, *FGFR1*, *FGFR2*, and *FGFR3*. Borderline significance ($P < 0.05$), when not accounting for multiple comparisons, was found for *FGF3*, *FGF7*, *FGF10*, *FGF18*, and *FGFR1* (Table 2). All *P* values are listed in SI Table 6. Additionally, a haplotype Family-Based Association Test was performed for pairs of SNP markers in genes. A significant *P* value of 0.009 was found for two *FGF3* markers (Table 2).

Gene × Gene Interaction. *FGF* and *FGFR* SNP genotypes were also used to perform gene × gene interaction studies. The most significant *P* values (≤ 0.0004) are listed in SI Table 7, and candidate genes in the interaction regions are indicated.

Discussion

Linkage, association, and sequencing are all useful and complementary approaches to providing evidence of a gene or gene family in disease. Sequencing (the primary approach reported here) is essential in cases where family structures limit linkage and there are no common variants present predisposing to disease. We used both sequencing and association to test whether the FGF gene family plays a role in clefting.

The FGF signaling pathway regulates multiple developmental processes, including craniofacial development. Evidence from previous work and the data presented here reveal that FGF signaling also plays an essential role in palatal development. When ascertainment bias was removed, we found a significant overrepresentation of missense mutations in the FGF gene family in cleft cases versus controls. The nine missense and nonsense mutations (Table 1) described in this paper may account for as much as 5% of NS CLP cases. Together with data from IRF6 (12%) (9); *FOXE1*, *GLI2*, *MSX2*, *SKI*, and *SPRY2* (6%) (6); and *MSX1* (2%) (7), these genes could account for $\leq 25\%$ of isolated clefting and have a significant impact on both the clinical diagnosis and genetic counseling of clefting in NS CLP. Importantly, structural analysis supports that at least three of the identified FGF and FGFR mutations negatively impact FGF signaling.

Table 2. Significant associations between FGF pathway genes and NS CLP

Markers	Allele	*P*
FGF3–1 rs4631909	2	0.04
FGF7–1 rs2413958	2	0.02
FGF10–1 rs1448037	2	0.01
FGF18–2 rs4073716	1	0.01
FGFR1–1 rs13317	1	0.03
FGF3–1 rs4631909, FGF3–2 rs4980700	2,1	0.009

The FGFR1 missense and nonsense mutations identified in this study demonstrate the nonpenetrance issues we face in identifying mutations in NS CLP. The R609X mutation was found in both father and daughter (Fig. 1); however, the daughter had KS, whereas the father had CLP with no additional phenotypes. The M369I mutation appears to segregate with the disease phenotype in the family (SI Fig. 6), yet there were unaffected family members with the mutation who may be examples of reduced penetrance. Evidence is emerging that some apparently nonpenetrant individuals in NS CLP families exhibit other phenotypic features, such as orbicularis oris muscle discontinuities that can be visualized by ultrasound, but this was not yet examined in these families (34). The E467K mutation is only found in one of two affected cousins (SI Fig. 6). It is possible that there is another gene that is modifying the effect of these FGFR1 mutations. Another possibility is that these mutations are modifying the effects of a second mutation elsewhere in the genome, possibly even with its heterodimerization partner FGFR2. It is clear that mutations in the FGFR1 gene have a role in clefting because 16 mutations have been previously identified in the coding region of the gene that are present in individuals with a syndromic form of clefting (KS) (SI Fig. 9) (15, 35–40).

The FGFR2 and FGFR3 mutations fall into critical protein domains that provide supporting evidence that these variants have functional significance. As previously proposed, for a mechanism of action in KS loss-of-function mutations, the R84S mutation in the D1 domain and the D138N mutation in the acid box domain of FGFR2 could accentuate the FGFR2 autoinhibition, thereby further repressing binding of FGF and heparin by the affected receptor (11). The D129A mutation in the acid box domain of FGFR1 results in autosomal-dominant KS with cleft palate as an additional phenotype (40), suggesting that mutations in this region of FGFRs may contribute to clefting. The V329I mutation in FGFR3 is predicted to result in a gradual unfolding of the D3 domain, and the affected FGFR3 protein is likely to be retained in the endoplasmic reticulum.

The FGF8 D73H mutation is the first example of mutations in the coding region of FGF8 in human disease. The patient with this *de novo* mutation appeared to have NS CLP with no additional phenotypes. Structural analysis shows that this is a definite case of a loss-of-function mutation. This mutation is predicted to reduce binding affinity of FGF8 toward its cognate receptors by both destabilizing the conformation of the FGF8 N terminus and directly eliminating hydrogen bonding with FGFRs.

Our association data demonstrate a trend toward association between *FGF*/*FGFR* genes and NS CLP, with several genes (*FGF3*, *FGF7*, *FGF10*, *FGF18*, and *FGFR1*) showing borderline significant values. When combined into a haplotype analysis, we see that the two markers in *FGF3* have a significant haplotype Family-Based Association Test *P* value. The *FGF3* gene is located on chromosome 11q13.3 and is immediately adjacent to

the *FGF4* gene, with ≈35 kb in between. We did not identify any mutations in the coding region of *FGF3* or *FGF4*, which would account for these *P* values; however, current projects are underway to sequence the noncoding conserved regions in and around these genes to look for variants in regulatory regions. Additionally, the gene × gene interaction data support both interactions between members of the FGF family, such as *FGF3* and *FGF18*, as well as interactions with other candidate genes that our laboratory is investigating, including *MSX2*, *EDN1*, and *PVRL1*.

Clinically, we can begin to think about creating sequencing screening panels by using the FGF and FGFR genes as well as other candidate genes, such as *IRF6*, *MSX1*, *MSX2*, *FOXE1*, *GLI2*, *SKI*, and *SPRY2*, which are highly likely to contribute to clefting. Such efforts are currently being pursued for early onset retinal degeneration (41), cystic fibrosis (42), and various cancer screening projects, including breast cancer (43), pediatric acute leukemia (44), and early cancer detection (45). Thus, the technology and high-throughput nature of this method will allow physicians and genetic counselors to test for mutations in known causative genes and enable carrier detection, prenatal screening, and improved recurrence risk estimates for other family members.

Biologically, knowing a quarter of the genes involved in clefting will help us to create models and pathways involved in clefting processes and help expand and look for additional pathways that may play a role. For example, sprouty (SPRY) 1 and 2 are downstream regulators of FGF signaling and have been previously examined for mutations in NS CLP patients (6). Three missense mutations were identified in SPRY2, two of which are potentially etiologic: D20A and K68N (6). SPRY genes antagonize FGF signaling through the regulation of the Ras/MAP pathway and have various biological consequences, including regulation of cell proliferation and differentiation (46). Future experiments will include mutational screening of upstream and downstream regulators of FGF signaling to define more precisely the FGF signaling pathway's contribution to lip and palate development.

Materials and Methods

Sample Collection. Ninety-one DNA samples from cases in the Philippines and another 93 from cases born in Iowa were sequenced in 84 amplicons (SI Table 3) for the following 12 genes: *FGFR1*, *FGFR2*, *FGFR3*, *FGF2*, *FGF3*, *FGF4*, *FGF7*, *FGF8*, *FGF9*, *FGF10*, *FGF18*, and *NUDT6*. The 184 cases are isolated, nonsyndromic unilateral cleft lip ($n = 1$), bilateral cleft lip ($n = 2$), unilateral CLP ($n = 60$) and bilateral CLP ($n = 102$), and CLP with unknown laterality ($n = 19$). Whole blood samples were collected by venipuncture. Subjects were reviewed by J.C.M. or S.D.-H. to exclude any with syndromic features and have been described in more detail in ref. 6.

Samples used for association studies came from work in conjunction with Operation Smile and Operation Smile–Philippines. Two hundred thirty Filipino families that had 2 or more affected members were collected; unaffected family members were collected as well. This set of Filipino samples was also used for genome-wide mapping approaches (47, 48). Clinical aspects of sample collection have been previously described (49, 50). The University of Iowa Institutional Review Board gave approval for sample collection (approval nos. 9701068, 199804081, and 200003065) in conjunction with local approval in the Philippines.

Sequencing. Cycle sequencing was performed in a 10-μl reaction by using 0.25 μl of ABI Big Dye Terminator sequencing reagent (version 1.1), 0.5 μl of 5 μM sequencing primer, 0.5 μl of DMSO, 1 μl of 5× buffer, and 6.75 μl of ddH_2O. Primers were designed from public sequence and are available on the Murray Laboratory web site at http://genetics.uiowa.edu. Following a denaturation step at 96°C for 30 sec, reactions were cycle sequenced at 96°C for 10 sec, 55°C for 5 sec, and 60°C for 4 min for 40 cycles. Cleanup occurred with magnetic beads by standard protocols and injected on an Applied Biosystems 3730 capillary sequencer (Applied Biosystems, Foster City, CA).

Sequence Analysis. Chromatograms were transferred to a Unix workstation (Sun Microsystems Inc., Mountain View, CA), base called with PHRED (version 0.961028), assembled with PHRAP (version 0.960731), scanned by POLYPHRED (version 0.970312), and the results viewed with the CONSED program (version 4.0) (51).

Genotyping and Statistical Analysis. Genotyping was carried out by using TaqMan Assays-on-Demand probes (Applied Biosystems) and done on an Applied Biosystems 7900 HT Sequence Detection System machine. Association studies were carried out by the Family-Based Association Test (32).

Gene × Gene Interaction Analysis. Linkage analyses were conducted by using our genome-wide linkage data from the Philippines population with the incorporation of covariates (FGF SNP genotypes) to detect interaction between loci by using the LODPAL program. Linkage parameters were first estimated under a base model without any covariates and then recalculated with each candidate locus included as a covariate (the SNPs for each FGF/R locus) (52). A region where the LOD score with a covariate significantly increased versus the base model was assumed to interact with the candidate locus (FGF/R) (52). The first analysis was done with 1,000 simulation steps; those that were significant ($P < 0.004$) were repeated with 10,000 simulation steps.

Alignments. Amino acid sequence alignments were made by using the CLUSTALW program. Accession numbers for the protein sequences were as follows: FGFR1: human NP 000595, chimp ENSPTRP00000034542, mouse NP 034336, rat XP 579483, chicken NP 990841, frog NP 001015894, and zebrafish NP 694494; FGFR2: human NP 000132, chimp ENSPTRP00000041191, mouse NP 034337, rat XP 341941, chicken NP 990650, and zebrafish NP 840088; FGFR3: human NP 000133, chimp XP 517065, dog XP 545926, mouse NP 032036, rat NP 445881, chicken NP 990840, and zebrafish NP 571681; FGFR4: human NP 998812; FGF8: human NP 149353, chimp ENSPTRP00000005056, rat NP 579820, mouse NP 034335, chicken NP 001012785, zebrafish NP 571356, and fugu NEWSINFRUP00000171015.

Structural Analysis of Mutations. The crystal structure of the FGFR1 tyrosine kinase domain [protein data bank identification (PDB ID): 1FGK] was used to investigate the effect of the E467K mutation (53). The effect of the V329I mutation in FGFR3 was studied by using the crystal structure of the complete extracellular region of FGFR3c in complex with FGF1 (PDB ID: 1RY7) (54). The effect of the D73H mutation in FGF8 was determined by analyzing the crystal structure of FGF8b in complex with the extracellular binding region of FGFR2c encompassing D2 and D3 (PDB ID: 2FDB) (30). The effect of the R84S mutation in D1 of FGFR2 was studied by using NMR structure of murine FGFR1 D1 (PDB ID: 2CKN) (29).

We thank all of the families who participated in this study; Susie McConnell, Dan Benton, and Melanie DeVore for their administrative assistance; and many other members of the Murray Laboratory, especially Brenna Trump, Marla Johnson, Temis Felix, and Fikre Menigstu, whose support and technical help were invaluable. This research was supported by National Institutes of Health Grants DE08559, DE16215, ES10876, and DE13686 (to M.M).

1. Lidral AC, Moreno LM (2005) *Curr Opin Pediatr* 17:731–739.
2. Jugessur A, Murray JC (2005) *Curr Opin Genet Dev* 15:270–278.
3. Christensen K, Juel K, Herskind AM, Murray JC (2004) *Br Med J* 328:1405–1407.
4. Berk NW, Marazita ML (2002) in *Cleft Lip and Palate*: *From Origin to Treatment*, ed Wyszynski DF (Oxford Univ Press, London), pp 458–467.
5. Schliekelman P, Slatkin M (2002) *Am J Hum Genet* 71:1369–1385.
6. Vieira AR, Avila JR, Daack-Hirsch S, Dragan E, Felix TM, Rahimov F, Harrington J, Schultz RR, Watanabe Y, Johnson M, *et al*. (2005) *PLoS Genet* 1:651–659.
7. Jezewski PA, Vieira AR, Nishimura C, Ludwig B, Johnson M, O'Brien SE, Daack-Hirsch S, Schultz RE, Weber A, Nepomucena B, *et al*. (2003) *J Med Genet* 40:399–407.
8. Suzuki Y, Jezewski PA, Machida J, Watanabe Y, Shi M, Cooper ME, Viet le T, Nguyen TD, Hai H, Natsume N, *et al*. (2004) *Genet Med* 6:117–125.
9. Zucchero TM, Cooper ME, Maher BS, Daack-Hirsch S, Nepomuceno B, Ribeiro L, Caprau D, Christensen K, Suzuki Y, Machida J, *et al*. (2004) *N Engl J Med* 351:769–780.
10. Ornitz DM, Itoh N (2001) *Genome Biol* 2:3005.
11. Mohammadi M, Olsen SK, Ibrahimi OA (2005) *Cytokine Growth Factor Rev* 16:107–137.
12. Slaney SF, Oldridge M, Hurst JA, Moriss-Kay GM, Hall CM, Poole MD, Wilkie AO (1996) *Am J Hum Genet* 58:923–932.
13. Park WJ, Theda C, Maestri NE, Meyers GA, Fryburg JS, Dufresne C, Cohen MM, Jr, Jabs EW (1995) *Am J Hum Genet* 57:321–328.
14. Kreiborg S, Cohen MM, Jr (1992) *J Craniofac Genet Dev Biol* 12:41–48.
15. Dode C, Levilliers J, Dupont JM, De Paepe A, Le Du N, Soussi-Yanicostas N, Coimbra RS, Delmaghani S, Compain-Nouaille S, Baverel F, *et al*. (2003) *Nat Genet* 33:463–465.
16. Dode C, Hardelin JP (2004) *J Mol Med* 82:725–734.
17. Kim HG, Herrick SR, Lemyre E, Kishikawa S, Salisz JA, Seminara S, MacDonald ME, Bruns GA, Morton CC, Quade BJ, *et al*. (2005) *J Med Genet* 42:666–672.
18. Entesarian M, Matsson H, Klar J, Bergendal B, Olson L, Arakaki R, Hayashi Y, Ohuchi H, Falahat B, Bolstad AI, *et al*. (2005) *Nat Genet* 37:125–127.
19. Rice R, Spencer-Dene B, Connor EC, Gritli-Linde A, McMahon AP, Dickson C, Thesleff I, Rice DP (2004) *J Clin Invest* 113:1692–1700.
20. De Moerlooze L, Spencer-Dene B, Revest J, Hajihosseini M, Rosewell I, Dickson C (2000) *Development (Cambridge*, *UK)* 127:483–492.
21. Ohbayashi N, Shibayama M, Kurotaki Y, Imanishi M, Fujimori T, Itoh N, Takada S (2002) *Genes Dev* 16:870–879.
22. Liu Z, Xu J, Colvin JS, Ornitz DM (2002) *Genes Dev* 16:859–869.
23. Trokovic N, Trokovic R, Mai P, Partanen J (2003) *Genes Dev* 17:141–153.
24. Abu-Issa R, Smyth G, Smoak I, Yamamura K, Meyers EN (2002) *Development (Cambridge*, *UK)* 129:4613–4625.
25. Cann HM, de Toma C, Cazes L, Legrand MF, Morel V, Piouffre L, Bodmer J, Bodmer WF, Bonne-Tamir B, Cambon-Thomsen A, *et al*. (2002) *Science* 296:261–262.
26. Klint P, Claesson-Welsh L (1999) *Front Biosci* 4:D165–D177.
27. Larsson H, Klint P, Landgren E, Claesson-Welsh L (1999) *J Biol Chem* 274:25726–25734.
28. Maquat LE, Carmichael GG (2001) *Cell* 104:173–176.
29. Kiselyov VV, Bock E, Berezin V, Poulsen FM (2006) *Protein Sci* 15:1512–1515.
30. Olsen SK, Li JY, Bromleigh C, Eliseenkova AV, Ibrahimi OA, Lao Z, Zhang F, Linhardt RJ, Joyner AL, Mohammadi M (2006) *Genes Dev* 20:185–198.
31. Asa SL, Ramyar L, Murphy PR, Li AW, Ezzat S (2001) *Mol Endocrinol* 15:589–599.
32. Horvath S, Xu X, Laird NM (2001) *Eur J Hum Genet* 9:301–306.
33. Rabinowitz D, Laird N (2000) *Hum Hered* 50:211–223.
34. Weinberg SM, Neiswanger K, Martin RA, Mooney MP, Kane AA, Wenger SL, Losee J, Deleyiannis F, Ma L, De Salamanca JE, *et al*. (2006) *Cleft Palate Craniofac J* 43:7–20.
35. Zenaty D, Bretones P, Lambe C, Guemas I, David M, Leger J, de Roux N (2006) *Mol Cell Endocrinol* 254–255:78–83.
36. Dode C, Fouveaut C, Mortier G, Janssens S, Bertherat J, Mahoudeau J, Kottler ML, Chabrolle C, Gancel A, Francois I, *et al*. (2007) *Hum Mutat* 28:97–98.
37. Pitteloud N, Acierno JS, Jr, Meysing A, Eliseenkova AV, Ma J, Ibrahimi OA, Metzger DL, Hayes FJ, Dwyer AA, Hughes VA, *et al*. (2006) *Proc Natl Acad Sci USA* 103:6281–6286.
38. Pitteloud N, Meysing A, Quinton R, Acierno JS, Jr, Dwyer AA, Plummer L, Fliers E, Boepple P, Hayes F, Seminara S, *et al*. (2006) *Mol Cell Endocrinol* 254–255:60–69.
39. Trarbach EB, Costa EM, Versiani B, de Castro M, Baptista MT, Garmes HM, de Mendonca BB, Latronico AC (2006) *J Clin Endocrinol Metab* 91:4006–4012.
40. Albuisson J, Pecheux C, Carel JC, Lacombe D, Leheup B, Lapuzina P, Bouchard P, Legius E, Matthijs G, Wasniewska M, *et al*. (2005) *Hum Mutat* 25:98–99.
41. Mandal MN, Heckenlively JR, Burch T, Chen L, Vasireddy V, Koenekoop RK, Sieving PA, Ayyagari R (2005) *Invest Ophthalmol Vis Sci* 46:3355–3362.
42. McGinniss MJ, Chen C, Redman JB, Buller A, Quan F, Peng M, Giusti R, Hantash FM, Huang D, Sun W, *et al*. (2005) *Hum Genet* 118:331–338.
43. Tennis M, Krishnan S, Bonner M, Ambrosone CB, Vena JE, Moysich K, Swede H, McCann S, Hall P, Shields PG, *et al*. (2006) *Cancer Epidemiol Biomarkers Prev* 15:80–85.
44. Mullighan CG, Flotho C, Downing JR (2005) *Cancer J* 11:268–282.
45. Maitra A, Cohen Y, Gillespie SE, Mambo E, Fukushima N, Hoque MO, Shah N, Goggins M, Califano J, Sidransky D, *et al*. (2004) *Genome Res* 14:812–819.
46. Tsang M, Dawid IB (2004) *Sci STKE* 228:1–5.
47. Marazita ML, Murray JC, Lidral AC, Arcos-Burgos M, Cooper ME, Goldstein T, Maher BS, Daack-Hirsch S, Schultz R, Mansilla MA, *et al*. (2004) *Am J Hum Genet* 75:161–173.
48. Schultz RE, Riley BM, Cooper ME, Goldstein T, Daack-Hirsch S, Lee KT, Dragan E, Magee W, Villanueva E, Vieira AR, *et al*. (2006) *Am J Hum Gene*, in press.
49. Schultz RE, Cooper ME, Daack-Hirsch S, Shi M, Nepomucena B, Graf KA, O'Brien EK, O'Brien SE, Marazita ML, Murray JC (2004) *Am J Med Genet A* 125:17–22.
50. Murray JC, Daack-Hirsch S, Buetow KH, Munger R, Espina L, Paglinawan N, Villanueva E, Rary J, Magee K, Magee W (1997) *Cleft Palate Craniofac J* 34:7–10.
51. Nickerson DA, Tobe VO, Taylor SL (1997) *Nucleic Acids Res* 25:2745–2751.
52. Brock G, Maher B, Goldstein T, Cooper M, Marazita M (2005) *BMC Genetics* 6(Suppl 1):S144.
53. Mohammadi M, Schlessinger J, Hubbard SR (1996) *Cell* 86:577–587.
54. Olsen SK, Ibrahimi OA, Raucci A, Zhang F, Eliseenkova AV, Yayon A, Basilico C, Linhardt RJ, Schlessinger J, Mohammadi M (2004) *Proc Natl Acad Sci USA* 101:935–940.